Hierarchical Structures Hot Paper

International Edition: DOI: 10.1002/anie.201503777
German Edition: DOI: 10.1002/ange.201503777

Step-by-Step Growth of Complex Oxide Microstructures**

*Panos Datskos, David A. Cullen, and Jaswinder Sharma**

Abstract: *The synthesis of complex and hybrid oxide microstructures is of fundamental interest and practical applications. However, the design and synthesis of such structures is a challenging task. A solution-phase process to synthesize complex silica and silica–titania hybrid microstructures was developed by exploiting the emulsion-droplet-based step-by-step growth featuring shape control. The strategy is robust and can be extended to the preparation of complex hybrid structures consisting of two or more materials, with each having its own shape.*

Marine organisms, such as sponges, produce spike-like structures from silicon and oxygen dissolved in the sea water.[1] It took sponges 800 million years of evolution to create these structures. Inspired by nature, scientists have synthesized several nano- and microstructures.[2,3] Among these structures, complex structures of oxides have always fascinated researchers working in materials science, biology, or engineering because of their implications in fields such as photonics, composites, and coatings (superhydrophobic, superhydrophilic, antireflective, antibiofouling, and antibacterial).[3] The easiest way to produce oxide structures is the layer-by-layer assembly of the building blocks,[4] however, this method only provides structures with isotropic (spherical) components. Structures can also be directly chiseled into diverse materials using lithographic techniques,[5] however, the lack of scalability, high cost, and low throughput hinder the further progress of lithography. Biomineralization-inspired approaches are also being explored to control the shape at the molecular level by techniques such as epitaxy. Though epitaxy has already been used in the growth of some intriguing structures,[6] the final shape is generally governed by the underlying structure, and it is hard to achieve structures of arbitrary shapes. Structures can also be produced by selectively depositing islands of one material on top of the other by partially covering the first material.[7] Similarly, colloidal oxide structures, such as particles, nanotubes, rods, and patchy particles, have been reported.[8] Recently, Aizenberg and co-workers reported that by manipulating the reaction conditions during the growth, structures of extraordinary morphologies can be obtained.[9] Despite the tremendous progress in the synthesis of these structures, the synthesis of complex structures of a single oxide and two or more oxides (hybrid structures) is still challenging.

Herein, we exploit the emulsion-droplet[8d]-based growth of anisotropic silica structures for the synthesis of a wide range of microstructures consisting of pure silica (silicon dioxide, SiO_2) and hybrid microstructures consisting of silica and titania (titanium dioxide, TiO_2). This approach provides a good control of 1) shape, 2) size, 3) number (less or more), and 4) composition of different parts of the structures.

Starting from a spherical particle, we synthesized complex SiO_2 structures, such as a central particle surrounded by smooth spikes, corrugated spikes, or plates. We further extended this strategy to the synthesis of hybrid complex microstructures comprised of one segment of titania and the other of silica. Many unprecedented structures, such as a silica double plate sandwiched between two particles, truncated triangle consisting of silica sandwiched in a particle trimer, and two silica-truncated triangles consisting of four plates sandwiched between a particle quadruple, were also obtained by the controlled deposition of silica.

In a typical preparation, preformed silica particles (600 nm) were first immersed in an aqueous polyvinylpyrrolidone (PVP; 14 mg PVP, 140 μL H_2O) solution in order to attach some PVP molecules to the particle surface. The attached PVP molecules acted as an initiation point for the attachment of emulsion droplets. In the second step, this aqueous solution containing PVP and particles was mixed with a solution of PVP (0.5 g) in pentanol (5 mL), followed by the addition of sodium citrate (0.18 M, 50 uL), ethanol (475 μL), and ammonium hydroxide (28–30%; 100 μL). Emulsion droplets consisting of PVP as interphase, citrate, water, and ammonium hydroxide as inner phase, and pentanol as outer phase, were attached to the particles (Supporting Information, Figures S1 and S2). The growth of spikes on the surface of the particles that had the emulsion droplets attached began with the addition of tetraethyl orthosilicate (TEOS) to the above-described solution. Initially, TEOS was hydrophobic in nature and resided in the pentanol phase. After penetrating through the PVP interphase, TEOS molecules were hydrolyzed and became hydrophilic, and a condensation reaction occurred inside the emulsion droplet, initiating spike growth. The spikes grew

[*] Dr. P. Datskos, Dr. J. Sharma
Nanosystems, Separations, and Materials Research Group
Energy and Transportation Science Division
Oak Ridge National Laboratory
One Bethel Valley Road, Oak Ridge, TN 37831 (USA)
E-mail: sharmajk@ornl.gov
Dr. D. A. Cullen
Material Science and Technology Division
Oak Ridge National Laboratory
One Bethel Valley Road, Oak Ridge, TN 37831 (USA)

[**] J.S. is a Research Staff at the Oak Ridge National Laboratory managed by UT-Battelle, LLC, for the U.S. Department of Energy under Contract DE-AC05-00OR22725. The work was supported by the Laboratory Director's Research and Development Program of the Oak Ridge National Laboratory. A portion of this research was conducted at the Center for Nanophase Materials Sciences, which is sponsored at Oak Ridge National Laboratory by the Scientific User Facilities Division, Office of Basic Energy Sciences, U.S. Department of Energy.

Supporting information for this article is available on the WWW under http://dx.doi.org/10.1002/anie.201503777.

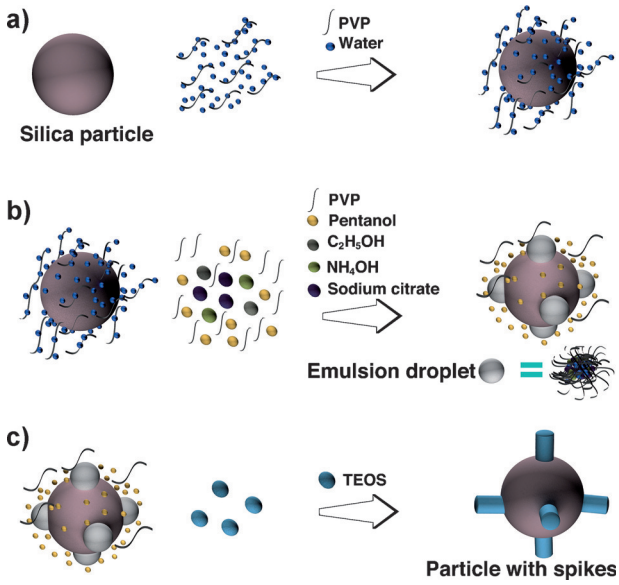

Figure 1. General procedure of the growth of complex silica structures. a) Attachment of PVP and water molecules to the surface of particles, b) addition of the solution obtained in step a to a solution of PVP in pentanol containing sodium citrate, ethanol, and ammonium hydroxide, and formation of the emulsion droplets, and c) addition of TEOS and growth of spikes.

wherever the emulsion droplets were attached to the particles. Figure 1 shows the general mechanism of spike growth on the surface of particles. Figure 2a shows scanning electron microscopy (SEM) images of the representative spiky structures, and Figure 2b shows the low-magnification SEM images of a sample. The actual length and diameter of the spikes depended upon the initial size of the emulsion droplet, that is, the smaller the emulsion droplet, the smaller the spike. We assume that small emulsion droplets had less water for hydrolysis of TEOS, and thus less silica was deposited. Detachment of the emulsion droplet during spike growth could also result in a small spike, as spike growth occurs only if the emulsion droplet is attached to the tip of the spike.

Though exact control of the spike length is difficult, the length could be controlled to some degree (from 50 nm to 2 μm) by manipulating the time allowed for spike growth. For example, Figure 2c shows structures with spike lengths of (i) 50 nm, (ii) 300 nm, and (iii) 1 μm, when spike growth was allowed for (i) 30 min, (ii) 2 h (hours), and (iii) 6 h. Figure 2d shows low-magnification SEM images of a sample when spikes were grown for (i) 30 min and (ii) 1 h. The size control of spikes indirectly led to a shape control, for example, small spikes look like plates (Figures 2c(i),2d(i), and S3).

A low particle concentration (140 μL of the stock solution; for details see the Supporting Information, Section S1 and Figure S4) produced more spikes on the particle surface, while a high particle concentration (280 μL of the stock solution) produced less spikes on particle surface (Figure S4). At a lower particle concentration, many spikes also grew alone in solution. When the particle concentration was too high (560 μL of stock solution), the growth of spikes at particle–particle junctions became predominant. This growth of spikes at the junction of two particles led to the

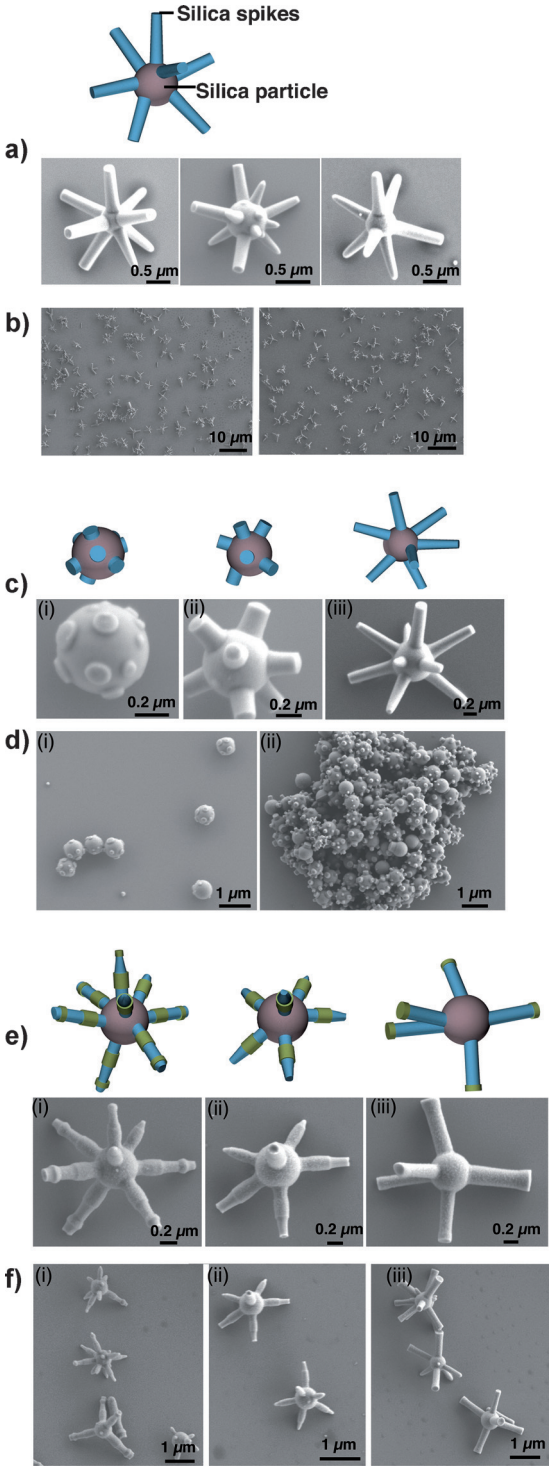

Figure 2. SEM images of spikes grown on silica particles. a) Images of some of the predominant structures; b) low-magnification images of the spiky structures; c) spikes grown for different time intervals [(i) 30 min, (ii) 3 h, and (iii) 6 h], d) low-magnification images of spikes grown for (ii) 30 min and (ii) 1 h, e,f) structures with corrugated spikes obtained by manipulating the reaction temperature while the spikes were growing; (i) 50°C (20 min), 4°C (3 h), 50°C (20 min), 4°C (3 h), 50°C (20 min); (ii) 50°C (20 min), 4°C (3 h), 50°C (20 min); and (iii) 50°C (10 min), 22°C (2 h), 4°C (5 h).

hypothesis that some of the particles could aggregate to form dimers and sandwiched the emulsion droplet, which led to spike growth at the junctions. Squeezed parts (Figure S5 b) of the spikes in the junctions indicate that the junction was formed before spike growth began. SEM imaging (Figure S5 a) after a few minutes of spike growth also showed the initiation of spike growth at the junctions, thus ruling out the possibility that particles sandwiched the preformed spikes.

To further increase the complexity of the structures and achieve better control of the spike shape, we exploited a temperature-induced change[8e] in the diameter of the spikes. Figure 2 f,g show the structures with corrugated spikes of different shapes when the temperature was systematically changed while the spikes were growing. During spike growth, an increase in the reaction temperature caused a decrease in spike diameter, and a decrease in temperature caused an increase in spike diameter. Combining the temperature-induced growth of corrugated spikes with preformed particles provided an unprecedented strategy for designing complex silica structures.

Several unprecedented morphologies, for example, a particle dimer sandwiching a double ring of silica, a particle trimer sandwiching a truncated triangle of silica, and a quadruple of silica particles sandwiching two truncated triangles of silica (Figure 3) were observed when the particle concentration was high (560 μL of stock solution) and spike growth was stopped after a few minutes. These structures were formed by initially sandwiching an emulsion droplet between two, three, and four particles, respectively. Either the particles were aggregated before the emulsion droplet was formed at the junction, or the particles sandwiched a preformed emulsion droplet. Both pathways could have given the same end products. The growth of two plate-like structures (in dimers) and four plate-like structures (in quadruples) shows that the silica deposition started from the edges, thus indicating a similar growth mechanism of spikes as explained by Kuijik et al. for the growth of silica rods.[8d] Figure 3 shows the bright-field scanning transmission electron microscopy (STEM) images of emulsion droplets sandwiched between particles, energy-dispersive X-ray spectroscopy (EDS) maps, and SEM images of the structures. EDS maps showed the presence of sodium (Na) in the emulsion droplets and silicon (Si) in silica particles. We chose the sodium of sodium citrate to ascertain the presence of emulsion droplets, because the intensity of nitrogen or carbon atoms of PVP was very low, and oxygen was present in both silica and PVP.

We further extended the above-described strategy to the synthesis of hybrid microstructures, for example, by using TiO_2 particles (550 nm) as seed, and growing the spikes as mentioned before; hybrid structures with a head of TiO_2 and spikes of silica were obtained (Figure 4). Compared to SiO_2 particles, fewer (usually one) spikes grew on TiO_2 particles. EDS maps showed that TiO_2 particles have a complete shell of an emulsion droplet, that is, a single droplet covering the whole particle (Figure S6). We assume that water got absorbed as a result of the higher hydrophilicity of TiO_2 particles, dispersed on the particle surface, and formed a single emulsion droplet per particle, and thus only one spike grew on each particle. In contrast to the TiO_2 particles,

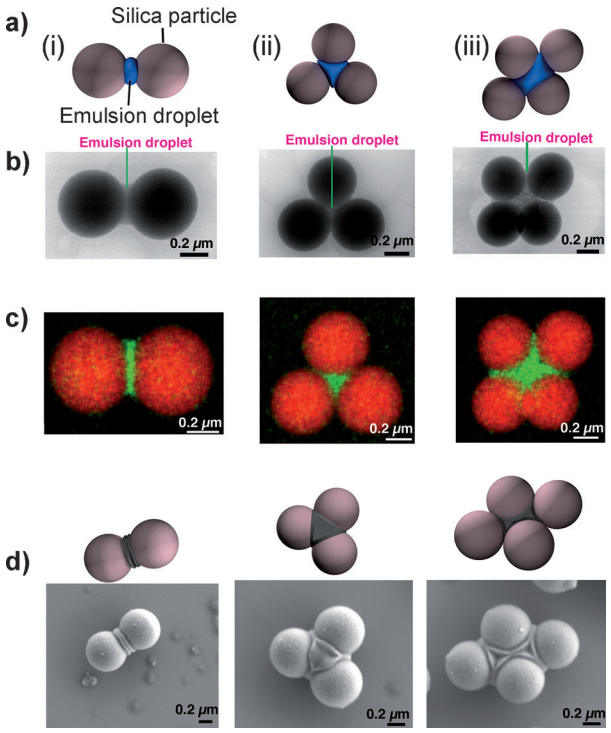

Figure 3. Growth of (i) a particle dimer sandwiching a double ring of silica, (ii) a particle trimer sandwiching a truncated triangle of silica, and (iii) a quadruple of silica particles sandwiching two truncated triangles of silica. a) Cartoons of the emulsion droplet sandwiched between two (i), three (ii), and four (iii) particles. b) STEM images showing the emulsion droplet sandwiched between two, three, and four particles. c) EDS maps showing the presence of Na from the emulsion droplet (green) Si from silica particles (red). d) Cartoons and SEM images showing a particle dimer sandwiching a double ring of silica, a particle trimer sandwiching a truncated triangle of silica, and a particle quadruple sandwiching two truncated triangles of silica. Note: All these structures were observed in a single sample and trimers and quadruple structures are less common.

individual emulsion droplets (more than one) attached to the silica particles, which resulted in multiple spikes per particle (Figure S6). A thin silica shell was formed between the particle and the spike (EDS and STEM images; Figure 4 (ii), (iii)), thus indicating that the shell was formed before any spike growth began. At higher TiO_2 particle concentrations, only a thick silica shell (no spikes) was formed around the TiO_2 particles (see Section S1 and Figure S7 in the Supporting Information). It appeared that at a higher particle concentration, an insufficient amount of water remained for further spike growth, and only a shell was formed. A lower particle concentration gave thick spikes ($d \approx 500$ nm), while the normal particle concentration gave thin spikes ($d \approx 300$ nm; Figure S8). This observation indicates that at lower particle concentration the amount of water and citrate available per particle was large (large emulsion droplet) and at higher particle concentration the amount of water and citrate available per particle was small (small emulsion droplet), that is, the emulsion droplets surrounding the particles at a lower particle concentration are bigger than those surrounding the particles at a higher particle concentration. The spike consisted of silica alone, while the head was

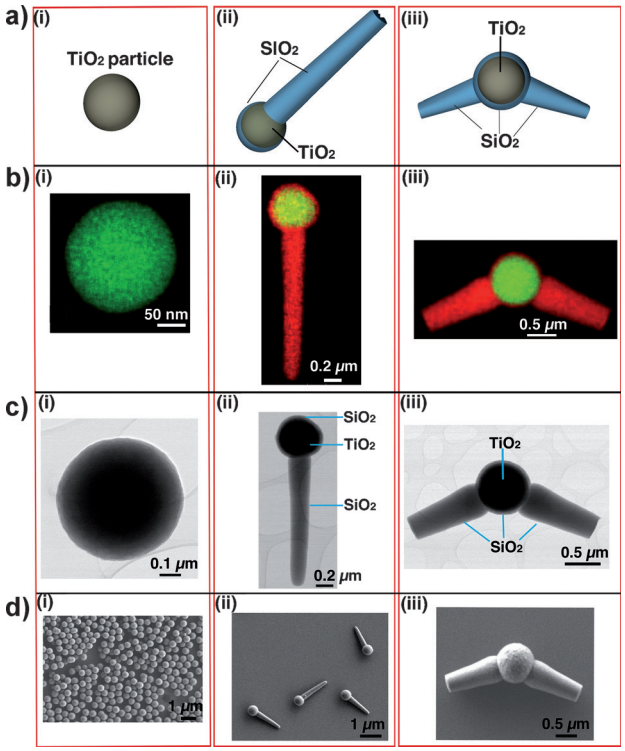

Figure 4. TiO_2–SiO_2 hybrid structures obtained by spike growth on TiO_2 particles. a) Cartoons, b) EDS maps (particle: green, spike: red), c) STEM images, and d) SEM images of (i) a sole TiO_2 particle, (ii) a TiO_2 particle with one spike, and (iii) a TiO_2 particle with two spikes.

hybrid (TiO_2 core and thin silica shell). An increase in TiO_2 particle size allowed growth of additional spikes ($\approx$550 nm one spike; Figure 4 a–c(ii) and $\approx$750 nm two or three spikes per particle Figure 4 a–c(iii) and Figure S9). It appears that the larger particles can attach to two emulsion droplets or emulsion droplet supported by larger particles can lead to two spikes. For TiO_2 particles, the control of the number (generally one) and length (50 nm –2 μm) of spikes is extremely good when compared to the spikes grown on silica particles. For example, more than 95% of 550 nm particles have one spike and less than 5% of these particles have either two spikes or none at all.

To further increase the complexity of the hybrid structures, we added (3-aminopropyl)triethoxysilane (APTES) to the TiO_2–SiO_2 head–spike structures, and obtained tricomponent [(APTES(head)-SiO_2(spike)-TiO_2(head)] hybrid structures (Figure 5). The addition of APTES led to a sphere at the spike end, where the emulsion droplet was attached. Because APTES is more reactive, quick deposition of silica occurred and a spherical shape was formed (see Section S1 in the Supporting Information). More SEM and EDS images of different structures discussed above are provided in the Supporting Information (Figures S10–S25).

In conclusion, we demonstrated an approach that can be employed to prepare a range of complex silica and silica–titania hybrid microstructures. Though not demonstrated in here, structures consisting of a TiO_2 head with corrugated spikes and a silica ring sandwiched between a dimer of TiO_2 particles can also be synthesized. We anticipate that this

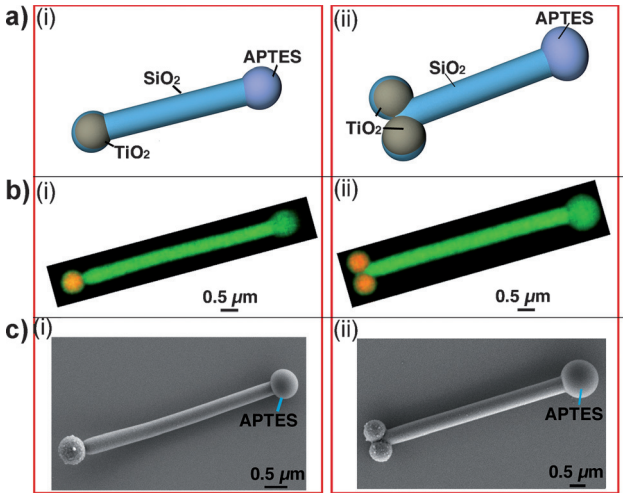

Figure 5. TiO_2–SiO_2 hybrid structures obtained by spike growth on TiO_2 particles. a) Cartoons showing (i) dumbbell-shaped structure consisting of a TiO_2 particle head on one end, a SiO_2 bridge, and an APTES head on the other end, (ii) dumbbell-shaped structure with two TiO_2 particles at either end; b) EDS maps of the structures shown in (a), TiO_2 head (orange), silica bridge (green), and APTES head (green). c) SEM images of the above-shown structures.

approach can be employed for the preparation of hybrid structures involving any hydrophilic seed particle, such as SnO_2, ZnO, Au, and Ag. For silica particles, an increase or decrease in the number and size of the spikes was easily achieved, even though it was difficult to exactly control these parameters. When TiO_2 particles were used as seeds, a better control of the exact number and size of the spikes was achieved. We anticipate that this work will open up opportunities for creating rationally designed complex structures with multiscale and hierarchical organization of constituting parts.

Keywords: hierarchical structures · hybrids · oxides · silica · titanium oxide

How to cite: *Angew. Chem. Int. Ed.* **2015**, *54*, 9011–9015
Angew. Chem. **2015**, *127*, 9139–9143

[1] a) M.-J. Uriz, X. Turon, M. A. Becerro, G. Agell, *Microsc. Res. Tech.* **2003**, *62*, 279–299; b) A. Pisera, *Microsc. Res. Tech.* **2003**, *62*, 312–326.
[2] a) A. R. Studart, R. M. Erb, *Soft Matter* **2014**, *10*, 1284–1294; b) E. Zhang, Y. Wang, T. Lv, L. Li, Z. Cheng, Y. Liu, *Nanoscale* **2015**, *7*, 6151–6158; c) Y. Hosseini, S. S. Verbridge, M. Agah, *J. Biomed. Mater. Res. A* **2015**, *103*, 2193—2197.
[3] a) D. Quéré, *Annu. Rev. Mater. Res.* **2008**, *38*, 71–99; b) S. Nishimoto, B. Bhushan, *RSC Adv.* **2013**, *3*, 671–690; c) L. Wen, T. Tian, L. Jiang, *Angew. Chem. Int. Ed.* **2015**, *54*, 2–15; *Angew. Chem.* **2015**, *127*, 2–2; d) C. K. Huang, K. W. Sun, W.-L. Chang, *Opt. Express* **2012**, *20*, A85–A93; e) Y. Li, J. Zhang, B. Yang, *Nano Today* **2010**, *5*, 117–127; f) W. Li, K. Lu, J. Y. Walz, M. Anderson, *J. Am. Ceram. Soc.* **2013**, *96*, 398–406.
[4] a) H.-J. Tsai, Y.-L. Lee, *Langmuir* **2007**, *23*, 12687–12692; b) C. H. Ho, G. J. Lin, P. H. Fu, C. A. Lin, P. C. Yang, I.-M. Chan, K. Y. Lai, J. H. He, *Sol. Energy Mater. Sol. Cells* **2012**, *103*, 194–198; c) X. Liu, J. He, *J. Phys. Chem. C* **2009**, *113*, 148–152.
[5] M. L. Brongersma, Y. Cui, S. Fan, *Nat. Mater.* **2014**, *13*, 451–460.

[6] a) S. Mann, *Nature* **1993**, *365*, 499 – 505; b) R. Gopikrishnan, K. Zhang, P. Ravichandran, S. Biradar, V. Ramesh, V. Goornavar, R. B. Jeffers, A. Pradhan, J. C. Hall, S. Baluchamy, G. T. Ramesh, *J. Mater. Sci. Mater. Med.* **2011**, *22*, 2301 – 2309.
[7] a) A. Perro, S. Reculusa, S. Ravaine, E. B. Lami, E. Duguet, *J. Mater. Chem.* **2005**, *15*, 3745 – 3760; b) Q. Chen, S. C. Bae, S. Granick, *Nature* **2011**, *469*, 382 – 385.
[8] a) Y. Liu, J. Goebl, Y. Yin, *Chem. Soc. Rev.* **2013**, *42*, 2610 – 2653; b) X. Yang, H. Tang, K. Cao, H. Song, W. Sheng, Q. J. Wu, *J. Mater. Chem.* **2011**, *21*, 6122 – 6135; c) J. Zhang, H. Liu, Z. Wang, N. Ming, *Chem. Eur. J.* **2008**, *14*, 4374 – 4380; d) A. Kuijk, A. V. Blaaderen, A. Imhof, *J. Am. Chem. Soc.* **2011**, *133*, 2346 – 2349; e) P. Datskos, J. Sharma, *Angew. Chem. Int. Ed.* **2014**, *53*, 451 – 453; *Angew. Chem.* **2014**, *126*, 461 – 464; f) P. Datskos, J. Chen, J. Sharma, *RSC Adv.* **2014**, *4*, 2291 – 2294; g) C. Gao, Z. Lu, Y. Yin, *Langmuir* **2011**, *27*, 12201 – 12208; h) J. Wang, A. Suguwara, A. Shimojima, T. Okubo, *Langmuir* **2010**, *26*, 18491 – 18498; i) D.-M. Li, Y.-C. Chen, C. Zhang, S. Song, Y.-S. Zheng, *J. Mater. Chem. B* **2013**, *1*, 1622 – 1627.
[9] W. L. Noorduin, A. Grinthal, L. Mahadevan, J. Aizenberg, *Science* **2013**, *340*, 832 – 837.

Received: April 24, 2015
Published online: June 10, 2015

